Functional characterisation of SiFPGS2 gene of foxtail millet in folates accumulation and root development

Yijuan Zhang
Shanxi Agricultural University
Chongmei Zhang
Shanxi Agricultural University
Xiaxia Man
Shanxi Agricultural University
Yihan Men
Shanxi Agricultural University
Xuemei Ren
Shanxi Agricultural University
Xueyin Li
Shanxi Agricultural University
Lida Han
Chinese Academy of Agricultural Sciences
Zhaoxia Sun
Shanxi Agricultural University
Yang Yang
Shanxi Agricultural University
Siyu Hou (✉ 18635068055@163.com)
Shanxi Agricultural University https://orcid.org/0000-0001-8341-6607
Yuanhuai Han
Shanxi Agricultural University

Research Article

Keywords: foxtail millet, SiFPGS2, folates content, root length, cell division.

Posted Date: July 19th, 2022

DOI: https://doi.org/10.21203/rs.3.rs-1841905/v1

Abstract

Folates content in foxtail millet (*Setaria italica*) are higher than that in major crops. Polyglutamylation of folates could enhance their compartmentalization, reducing their transport, increase their affinities with enzymes and increase the stability of the folates pool in *Arabidopsis*. The polyglutamylation reaction are catalyzed by folylpolyglutamate synthetase (FPGS). But FPGS function in foxtail millet is still elusive. In this study we identified *Setaria italica FPGS2* (*SiFPGS*2) genes in foxtail millet by blast analysis with AtFPGS1/2/3 protein sequences. The phylogenetic tree analysis, protein function domain analysis and docking analysis results showed that SiFPGS2 belong to FPGS subfamily, possessed the tetrahydrofolypolyglutamate synthase domain, could bind tetrahydrofolate (THF) as substrate. Subcellular localization predicted that SiFPGS2 localized in the chloroplast. Cis-acting elements prediction analysis indicated that there were meristem expression motif and root specific motif in *SiFPGS2* promoter. Over-expressed *SiFPGS2* in *Arabidopsis* not only increased the folates content, but also increased the root length, and further propidium iodide staining result suggested that the increased root length was owning to the promotion of cell division in root apical meristem zone. SiFPGS2 catalyzed the polyglutamylation of THF and lead to the increase of folates content and root length by promotion of root apical meristem zone cell division. *SiFPGS2* can be used as a candidate gene for biofortification of folates in Gramineae crops via genetic engineering.

Summary

It is concluded that (i) SiFPGS2 possessed the tetrahydrofolypolyglutamate synthase activity, catalyze polyglutamylation of THF, and (ii) over expressed *SiFPGS2* in *Arabidopsis* not only increased the folates content by improving their stability, but also increased the root length by promotion of cell division in root apical meristem zone. The results of this study suggested that *SiFPGS2* can be used as a candidate gene for biofortification of folates in Gramineae crops via genetic engineering.

Introduction

Folates contain tetrahydrofolate and its derivatives, constitute vitamin B9, mediate the transformation of one-carbon (C1) units, also referred to as C1 metabolism, which participates in the synthesis of purines, thymidylate, methoine, pantothenate, and in the methyl group conversion between glycine and serine (Hanson and Roje 2001, Jagerstad and Jastrebova 2013). According to the C1 units attached at the N-5 or N-10 positions, folates form a lot of deviratives, such as 5-methyltetrahydrofolate (5-CH_3-THF), 5-formyltetrahydrofolate (5-CHO-THF), 10-formyl-THF (10-CHO-THF), 5,10-methylene-THF (5,10-CH = THF) and THF (Gorelova et al. 2017). Plants, funguses and bactierias can synthesis folates de novo, human and animals could not synthesis by themselves and have to rely on daily dietary (Scott et al. 2000). The recommended daily allowance (RDA) of folates are 400 μg for a common adult and 600 μg for a pregnant woman (Hou et al. 2022a). It is well known that inadequate intake of folates will lead to neural

tube defects (NTDs) in fetus and megaloblastic anemia, and will increase the risk of cardiovascular and coronary diseases and several types of cancer (Gregory and Quinlivan 2002, Mcnulty et al. 2019).

Folates are composed of three parts, pterin, p-aminobenzoic acid (p-ABA) and glutamate tail, which are produced separately in cell and then joined together. The pterin moiety is catalyzed by a series of enzymes from guanosine triphosphate (GTP) in the cytosol and the p-ABA moiety is catalyzed by two-step enzymatic reactions from chorismate in the plastid. Pterin and p-ABA are then transported to the mitochondria, where they are coupled together to form dihydropteroate (DHP). The first glutamic acid is added to dihydropteroate to produce dihydrofolate (DHF), following that, DHF is reduced to THF (Ravanel et al. 2001). Lastly, part of THF could be transported to platid, vacuole and cytosol, and the γ-linked glutamates could be added to the last glutamate in mitochondria, plastid, vacuole and cytosol, producing folate polyglutamates (Strobbe and Van Der Straeten 2017, De Lepeleire et al. 2018). Polyglutamylated folates are the predominant form of folates in all organisms. Usually, they are compartmentalized and show restricted intercellular and interorganellar movement. In addition to reducing transport, polyglutamylation could increase the association with folate-dependent enzymes, which typically have higher affinities for polyglutamylated folates than for mono- or di-glutamyl derivatives (Besson et al. 1993, Eckermann et al. 2000). Meanwhile the association of polyglutamylated folates with enzymes could increase the stability of the folates pool (Orsomando et al. 2005, Blancquaert et al. 2015).

In organisms that synthesize tetrahydrofolate de novo, dihydrofolate synthetase (DHFS/DFA/GLA1) and folylpolyglutamate synthetase (FPGS, contains DFB, DFC and DFD) catalyze the attachment of glutamate residues to the folate molecule. DHFS catalyze the first glutamate to DHP to yield DHF. In *Arabidopsis*, DFA was present exclusively in the mitochondria, *dhfs/dfa/gla1* mutant developed normally in the early stage of development but did not undergo the transition to the heart stage, which indicated that DFA was essential for embryogenesis in *Arabidopsis* (Ravanel et al. 2001, Ishikawa et al. 2003).

AtFPGS1/2/3, also known as AtDFB/C/D, the enzymes that catalyze the addition of glutamate residues to the folate molecule to form folylpolyglutamates, localized in the mitochondria, cytosol and chloroplast, respectively. The mutant in *Atfpgs* genes would change the ratio between poly-glutamated folates and mono-glutamated folates, disrupt folate polyglutamylation homeostasis, affect the organism development. In *Arabidopsis*, biochemical analysis of single *fpgs* loss-of-function mutants established that folate polyglutamylation was essential for organellar development and whole-plant folate homeostasis (Mehrshahi et al. 2010). *Atfpgs1/Atdfb* muatnt showed short primary root phenotype, associated with a disorganized quiescent center, dissipated auxin gradient in the root cap, bundled actin cytoskeleton, and reduced cell division and expansion (Srivastava et al. 2011a). Meanwhile, *Atfpgs1/Atdfb* mutant decreased DNA methylation in the direct repeats of *Flowering Wageningen* (*FWA*) gene region and exhibited significant up-regulation of the flowering repressor of *FWA* and thereby delayed floral transition in a dose-dependent manner (Wang et al. 2017). *FPGS* showed gene redundancy in *Arabidopsis*, *fpgs1 fpgs2* double mutants were embryo-lethal, *fpgs2 fpgs3* mutants exhibited seedling lethality, and *fpgs1 fpgs3* mutants were dwarfed with reduced fertility (Mehrshahi et al. 2010). The results above indicated that FPGS played important roles in organism development.

Foxtail millet (*Setaria italica)*, a minor yet important crop, shows strong adaptability to abiotic stresses, especially drought and poor soil, is cultivated in some drought and semi-drought areas of the world, particularly northern China (He et al. 2015). The publishments of many foxtail millet cultivars genome sequences and the discovery of model C4 plant species foxtail millet mutant *xiaomi*, provided the enormous convenience for the research of foxtail millet (Bennetzen et al. 2012, Zhang et al. 2012, Yang et al. 2020). Hulled grain of foxtail millet is rich in nutrients including essential amino acids, fatty acids, minerals and vitamines (Sachdev et al. 2021).Compared to the major crops, foxtail millet is rich of folates. The folate content in foxtail millet (1.6 $\mu g \cdot g^{-1}$) were about 2 to 5 times than in wheat (0.8 $\mu g \cdot g^{-1}$) and rice (0.3 $\mu g \cdot g^{-1}$), respectively (Shao and Wang 2014). Howerver, the research about folates in foxtail millet is limited to date. In the early years, most of the researches were focused on the extraction and measurement of folates in foxtail millet (Shao et al. 2014, Man et al. 2020). Recently, several reports focus on the folate accumulation mechanism in foxtail millet. Hou *et al* assessed the relationship between folate metabolites, the expression patterns of folate metabolism-related genes and folate synthesis, accumulation during panicle development in foxtail millet (Hou et al. 2022a), revealed SiFBP (*Setaria italica* folate binding protein) could improve folates and amino acids metabolism (Hou et al. 2022b).

In this study, we identified *SiFPGS2* in foxtail millet by blast analysis, predicted its function by docking analysis, subcellular localization analysis and promoter analysis, the results suggested that SiFPGS2 was highly homologue to SiFPGS1 and possessed the tetrahydrofolypolyglutamate synthase activity, SiFPGS2 protein construction was fit for binding THF as substrate, SiFPGS2 localized in the chloroplast and maybe take part in the root meristem development. SiFPGS2 over-expressed in *Arabidopsis* further verified that SiFPGS2 could increase folate content and promote major root development by accelarating meristem zone cell division. Our findings provide new insights and potential targets for breeding folate-rich foxtail millet cultivars.

Materials And Methods

Plant materials

The foxtail millet germplasm YuGu1 was collected from Shanxi Key Laboratory of Germplasm Innovation and Molecular Breeding of Minor Crop. They were planted in the field at Taigu district of Shanxi province. Their leaves of the foxtail millet seedlings were collected at 15 days after sowing (DAS) and storage at -80℃ waiting for RNA extraction. The *Arabidopsis* seeds were surface sterilized with bleach, then they were sown on $^1/_2$ MS solid plate with 1% sucrose and grown in a white light chamber with a photoperiod of 16/8 h (day/night) and a temperature of 22℃. For root length measurement, the seedlings were first scanned and the root length was measured on scanned images using Scion Image.

Bioinformation analysis of gene function

Three SiFPGS proteins were obtained from foxtail millet by using blast analysis in the phytozyme (https://phytozome-next.jgi.doe.gov) with related *Arabidopsis* protein sequence. Then the other protein sequence used for phylogenetic tree analysis was collected from NCBI by blasts with SiFPGS1, SiFPGS2, SiFPGS3, respectively. The unrooted phylogenetic tree was drawn based on the alignment with the MEGA software. A neighbour joining tree based on the conserved region was shown. Sequences used here are available in phylogenetic tree data. The protein conserved domain analysis, the promoter analysis and the subcellular localization were predicted by the online analysis tools Cyclic Delay Diversity (https://www.ncbi.nlm.nih.gov/cdd/), PlantCARE (http://bioinformatics.psb.ugent.be/webtools/plantcare/html/) and ProtComp (http://linux1 softberry com), respectively.

Docking analysis

Firstly, THF ($C_{19}H_{23}N_7O_6$, Pubchem SID:3401, Pubchem CID:135398650) and DHP ($C_{14}H_{14}N_6O_3$, Pubchem SID:4175, Pubchem CID: 135398662) chemistry constructions were downloaded from pubmed database (https://pubchem.ncbi.nlm.nih.gov/) to construct the ligand library modeling, the files were opened with AutodockTools1.5.6, the electricity charge and hydrogen atoms were added to THF and DHP, respectively. Then the ligands root was tested, the rotatable bond was definition and found, saved as pdbqt files. Subsequently, the protein structions were downloaded from I-TASSER (https://zhanggroup.org//I-TASSER/), then the file was opened with AutodockTools1.5.6 and saved as pdbqt. All the hydrogen atoms were added to the proteins, the nonpolar hydrogen were combined together, and electricity charge was calculated by gasteiger. Then docking simulation was performed in Autodock Vina 1.1.2. The construction with best affinity and the lowest binding energy between the protein and ligand was chosen as the docking construction. The docking result was analyzed by Pymol and Ligplot software.

Transgenic lines

For *35S::SiFPGS2*/Col-0 over-expression lines, the coding DNA sequence (CDS) of *SiFPGS2* gene under the control of a *35S* promoter was cloned into a pART-CAM vector using the seamless-cloning method. Firstly, *SiFPGS2* CDS was amplified using TransStart® FastPfu DNA Polymerase (TransGene Biotech Co., Ltd. CAS No. AP221-01) with gene-specific primers added 15 bp of nucleotides that were homologous to the vector restriction sites, the forward primer: 5’-GAGGACACGCTCGAGATGCCGCG

AAGCGGCGCCCGTG-3’, the reverse primer: 5’-TAAAGCAGGACTCTAGATTAC

TTCTTGATAAGCCTCAAGACA-3’. Subsequently, the empty vector was digested with restriction enzymes XhoI and XbaI. Then the amplified PCR products were ligazed to the digested vector with ClonExpressII One Step Cloning Kit (Vazyme Biotech Co., Ltd. CAS No. C112). After sequencing, the vector was transformed into *Arabidopsis* by the *Agrobacterium tumefaciens* GV3101 mediated floral-dip method. T_1-generation over-expression lines of *Arabidopsis* were verified by genomic PCR, the forward primer: 5’-AGCACAGATTGTTCCAGATTCA-3’, the reverse primer: 5’-AGGATCT

GAGCTACACATGCTC-3', T_3-generation transgenic lines with high expression level were chosen by quantitative real-time PCR and further analysed, the forward primer: 5'-CGCAGGCAGGGGGGATTTCAG-3', the reverse primer: 5'-GCATGTCGAACCCTTCC

CCTTGG-3'.

Folate measurement

The folates extraction protocol and measurement were performed as previously described with slight modification (Wan et al. 2019, Hou et al. 2022a). The fifth-seventh leaves of *Arabidopsis* grown in the plant culture room for one month old were harvest from fifteen independent plants to examine folate metabolites. Folate standards, 5-CH_3—THF, 5-CHO—THF, 5,10-CH□THF, DHF and THF were purchased from Schircks Laboratories (Jona, Switzerland). Methanol used for dissolution the folate standards were obtained from Thermo Fisher Scientific (Geel, Belgium). Formic acid and acetonitrile for high-performance liquid chromatograph-tandem mass were ordered from Thermo Fisher Scientific (Geel, Belgium).

All samples were oven dried at 80°C to a constant weight, ground into powder using an MM400 mixer mill (Retsch, Haan, Germany) with 30 Hz for 1.5 minutes. Fifty mg powder was dissolved in 1 mL freshly prepared extraction buffer (50 mM phosphatebuffered saline, pH 7.0, containing 0.5% (w/v) L-ascorbic acid, 0.2% β-mercaptoethanol and 20 $ng \cdot mL^{-1}$ methotrexate (MTX)), mixed and boiled for 10 minutes and cooled to room temperature in ice. Then 20.0 μL α-amylase (40 mg/ml) was added to the reaction liqiud, vortexed for 40 s and digested at 37°C for 30 minutes with softly shaken, bolied for 5 minutes to inactivate the α-amylase and cooled in ice. After this, the rat serum was added and the mixture was digested for 4 hours at 37°C, boiled for 5 minutes and cooled in ice for 10 minutes. The extracted sample was centrifuged at 15000 g for 10 minutes. After centrifuge, purified the supernatant with 3 kDa ultrafiltration tube and 15.0 μL filtered liqiud was used to perform the Ultra High-Performance Liquid Chromatograph (UHPLC, Agilent 1290)-tandem Mass Spectrometer (MS/MS, Agilent 6420) system for folate analysis.

The Agilent 1290 UHPLC system with an Agilent analytical column (Kromasil 100-5C18, 2.1 × 50 mm) was used for chromatographic analyses. The solution 0.1% (v/v) formic acid in ultra pure water (phase A) and 0.1% (v/v) formic acid in acetonitrile (phase B) were used as the mobile phases.The propotion of mobile phase B increased from 5 to 9% in 2 minutes, then phase B linearly increased to 9.5% in the following 5.9 minutes, then sharply increased to 20% in 0.3 minutes and holding at 20% for 3 minutes. Subsequently, the phase B linearly decreased to 5% in 0.2 minutes and holding at 5% for 0.1 minutes.

Propidium iodide staining and confocal

Propidium iodide (PI) staining was performed as previously described (Zhang et al. 2016), *Arabidopsis* major root grown in chamber four days old were stained with 180 μM PI directly, then imaged using confocal laser scanning microscope (Leica SP8, Germany) with the excitation wavelength at 540 nm.

RNA extraction and quantitative real-time PCR (qRT–PCR) analysis

The leaves of YuGu1 grown in the field for 15 days were collected in liquid nitrogen waiting for RNA extraction to amplify the CDS. The seedliongs of wild type (Col-0) and transgenic plants grew in culture room for 7 days were harvested for chosen of over-expression lines. Total RNAs of the samples were extracted using an *EasyPure*® Plant RNA Kit (TransGene Biotech Co., Ltd., CAS No.ER301) according to the manufacture's instructions. One microgram total RNA was reverse transcribed to cDNA by a PrimeScript™ RT reagent Kit with gDNA Eraser kit (Takara Biomedical Technology Co., Ltd., CAS No.RR047A) according to the manufacturer's instructions. Then the transcribed production was diluted according to the ratio of 1:20. qRT-PCR analysis was carried out using ChamQ Universal SYBR qPCR Master Mix (Vazyme Biotech Co., Ltd. CAS No.Q711-02) with CFX96 Real-Time System (Bio-Rad, USA). Each reaction mixture consisted of 9.6 μL diluted cDNA template, 10.0 μL 2× ChamQ Universal SYBR qPCR Master Mix, and 0.4 μL of each forward primer (10 μM) and reverse primer (10 μM). A 40-cycle, three-step amplification protocol (5 seconds at 94°C, 15 seconds at 56°C and 10 senconds at 72°C) was used for all measurement. The gene relative expression level was caculated by $2^{-\Delta\Delta Ct}$ method. Primers used for qRT-PCR were as below: *SiFPGS2*-RT-F, 5'-CGCAGGCAGGGGGGATTTCAG-3', *SiFPGS2*-RT-R, 5'-GCATGTCGAACCCTTCCCCTTGG-3'; *REF3*-RT-F, 5'- GGAGCCAACTAGGACGGATCTGG-3', *REF3*-RT-R, 5'-GTAGATCAATCCCAA

TAACCTGGTTCACTT-3', REF3 (*at1g13320*), which renamed as *PP2A* was used as reference gene (Yu et al. 2015).

Results

Phylogenetic analysis of SiFPGS and protein function domain prediction

According to homology-type research strategy, three SiFPGS proteins were obtained from foxtail millet by using blast analysis in the phytozyme (https://phytozome-next.jgi.doe.gov), which were renamed as SiFPGS1, SiFPGS2 and SiFPGS3, respectively. The phylogenetic tree analysis result revealed that the three SiFPGS proteins were classified into 2 subclades, SiFPGS1 and SiFPGS2 were homologue to each other and closely related to other FPGS1 and FPGS2 from some gramineae species like SvFPGS (*Setaria viridis*), SbFPGS (*Sorghum bicolor*), ZmFPGS (*Zea mays*) and OsFPGS (*Oryza sativa*), respectively, whereas SiFPGS3 was related to DFA from other species. In addition, FPGS in the dicots, such as GmFPGS1 (*Glycine max*), GmFPGS2 (*Glycine max*), SlFPGS1 (*Solanum lycopersicum* L.), AtFPGS1 (*Arabidopsis thaliana*) and AtFPGS3 composed another subclade, only AtFPGS2 belong to a independent subclade (Fig. 1). The protein function domain analysis was performed in the online software Cyclic Delay Diversity (https://www.ncbi.nlm.nih.gov/cdd/) and the results showed that SiFPGS1and SiFPGS2

possessed tetrahydrofolypolyglutamate synthase domain PLN02881 at 75–589 aa and 86–579 aa, respectively, while SiFPGS3 had dihydrofolate syhthase domain PLN02913 at 17–558 aa (Fig. S1).

Docking analysis

To determine whether SiFPGS1, SiFPGS2 could bind THF as substrate, and SiFPGS3 could bind DHP as substrate, the molecular docking analysis was taken on. It was predicted that SiFPGS1 and SiFPGS2 had the lowest binding energy of -9.6 kcal·mol^{-1} and − 9.2 kcal·mol^{-1} with THF, respectively, SiFPGS3 had the lowest binding energy of -8.7 kcal·mol^{-1} with DHP. THF had a strong hydrophobic interaction with Pro^{173}, Thr^{154}, Ser^{151}, Thr^{171}, Gly^{150}, Lys^{147}, Glu^{180}, Ser^{172}, His^{340}, Ser^{422}, Ala^{390}, Cys^{385}, Cys^{426}, Asp^{415} and an electrostatic interaction with Cys^{385} of SiFPGS1. Three hydrogen bonds holding the SiFPGS1 to THF were formed at Arg^{183}, Gln^{387}, Arg^{389} with a 2.91 Å, 2.89 Å, 3.04 Å, respectively (Fig. S2a). Similarly, THF had a strong hydrophobic interaction with Ile^{417}, Ala^{409}, Ser^{414}, His^{334}, Gly^{144}, Arg^{175}, Pro^{167}, Glu^{174}, His^{168}, Gln^{381}, Ser^{166}, Leu^{169}, Leu^{380} and an electrostatic interaction with Asp^{407} of SiFPGS2. Five hydrogen bonds holding the SiFPGS2 to THF were formed at Lys^{141}, Trp^{421}, Arg^{383}, Glu^{235}, Thr^{165} with a 3.06 Å, 3.12 Å, 3.17 Å, 3.05 Å, 3.12 Å, respectively (Fig. 2). DHP had a strong hydrophobic interaction with Ser^{119}, Gly^{387}, Arg^{363}, Ser^{393}, Pro^{121}, Lys^{97}, His ^{324}, Leu ^{123}, Gly ^{98}, Leu ^{360}, Pro ^{361}, Lys ^{95} of SiFPGS3 and an electrostatic interaction with Glu^{191}, the hydrogen bond holding the SiFPGS3 to DHP was formed at Gly^{96} with a 2.96 Å (Fig. S2b). The results revealed that SiFPGS1, SiFPGS2 could dock with THF, SiFPGS3 could dock with DHP, which suggested that SiFPGS1, SiFPGS2 protein conformation were fit for binding THF as substrate, while SiFPGS3 protein conformation was fit for binding DHP as substrate.

Subcellular prediction analysis and promoter prediction analysis

Further, we predicted SiFPGSs protein subcellular localization by ProtComp software (http://linux1 softberry com), and the results showed that SiFPGS1 scored of 5.61, 4.25, 0.1, 0.04 in the chloroplast, cytoplasm, extracellular and cell membrane, respectively. Similarly, SiFPGS2 scored of 5.57, 4.24, 0.13 and 0.04 in the chloroplast, cytoplasm, extracellular and cell membrane, respectively. However SiFPGS3 made a score of 2.36, 2.14, 1.31, 1.29, 1.20, 1.09. 0.61 and 0.04 in extracellular, peroxisome, mitochondria, chloroplast, golgi apparatus, endoplasmic reticulum, cytoplasm and cell membrane, respectively (Table 1). The result revealed that SiFPGS1, SiFPGS2 made the highest score in the chloroplast, SiFPGS3 made the highest score extracellular, which suggested that maybe SiFPGS1, SiFPGS2 localize in the chloroplast, and SiFPGS3 localize extracellular.

Table 1
Subcellular localization analysis of SiFPGS proteins

Subcellular location	Integral		
	SiFPGS1	SiFPGS2	SiFPGS3
Cytoplasm	4.25	4.24	0.61
Chloroplast	5.61	5.58	1.29
Extracellular	0.10	0.13	2.36
Peroxisome	0.00	0.00	2.14
Nucleus	0.00	0.00	0.00
Mitochondria	0.00	0.00	1.31
Endoplasmic reticulum	0.00	0.00	1.09
Golgi apparatus	0.00	0.00	1.20
Cell membrane	0.04	0.04	0.04
Vacuole	0.00	0.00	0.00

To further predict which signal pathway SiFPGSs may take part in, cis-acting element prediction analysis was carried on, and the result showed that the three genes shared the common necessary core elements, such as light response element (TCT-motif), MeJA response element (CGTCA-motif), anaerobic induction element (ARE motif) and abscisic acid response element (ABRE motif). *SiFPGS1* specially possessed defense and stress response element (TC-rich repeats motif), seed-specific regulation element (RY-motif); *SiFPGS2* specially possessed root specific element (motif I), meristem expression element (CAT-box motif); *SiFPGS3* specially possessed low temperature responsive element (LTR motif) and anoxic specific inducibility element (GC-motif) (Fig. 3, Table 2).

Table 2
Cis-acting elements analysis of *SiFPGS* genes family of foxtail millet

cis-acting element		Position		
		SiFPGS1	SiFPGS2	SiFPGS3
light response element	TCT-motif	1060, 1079	55, 665, 885, 988, 1157, 1640	411, 623, 973, 1139, 1225, 1313, 1743, 1834
MeJA response element	CGTCA-motif	1337, 1431	1223, 1676	45, 637, 1185, 1285
anaerobic induction element	ARE motif	1301, 1977	444, 1025, 1945	1724
abscisic acid response element	ABRE motif	769	1678	363, 1120, 1121, 1124, 1187
gibberellin response element	GARE motif	1576	854, 1987	-
salicylic acid response element	TCA-motif	-	1401,1420,1899, 1914	1711
zein metabolism regulation element	O2 motif	-	1498	1180, 1188
defense and stress response element	TC-rich repeats motif	1083	-	-
seed-specific regulation element	RY-motif	867	-	-
meristem expression element	CAT-box motif	-	1001, 1750	-
root specific element	motif I	-	1174	-
anoxic specific inducibility element	GC-motif	-	-	118
low temperature response element	LTR motif	-	-	1020

Over-expression SiFPGS2 **gene in** Arabidopsis **increased folates content**

The phylogenetic tree analysis,the protein function analysis and docking analysis results suggested that SiFPGS1, SiFPGS2 homologue to each other and possessed the tetrahydrofolypolyglutamate synthase activity, belong to FPGS family; whereas,

SiFPGS3 was similar to DFA subfamily and possessed dihydrofolate synthase activity. Subcellular localization predicted that SiFPGS1, SiFPGS2 localized in the choloroplast, SiFPGS3 localized extracellular. Taken together, the bioinformation assays indicated that SiFPGS1 was homologue to

SiFPGS2, while SiFPGS3 belong to DFA family, in the following research we choose *SiFPGS2* as target gene to avoid gene redundancy. To further detect the gene function, *SiFPGS2* were over-expressed in *Arabidopsis*, the transgenic lines were verified by genomic PCR (Fig. S3a), and the lines with highest expression level #3, was chosen out by qRT-PCR (Fig. S3b). The 5th -7th leaves one month old of wild type and over-expression lines were harvested and the folates content were measured, respectively, and the result showed that 5-CH_3-THF, 5-CHO-THF, 5,10-CH = THF and THF content in wild type was 43.40, 6.06, 47.81, 8.04 μg·100g^{-1}, they were increased to 51.12, 6.24, 53.31, 9.23 μg·100g^{-1} in *SiFPGS2* over-expression line, respectively, which suggested that over-expression of *SiFPGS2* could increase the THF and its derivatives content; whereas in *SiFPGS2* over-expression line DHF was decreased to 0.75 μg·100g^{-1} compared to 1.83 μg·100g^{-1} in wild type (Fig. 4).

Over-expression SiFPGS2 **in** Arabidopsis **promote root growth**

It was reported that *Atdfb/Atfpgs1* mutant show a short root phenotype (Srivastava et al. 2011b), above result showed that SiFPGS1, SiFPGS2 and AtFPGS1, AtFPGS2 possessed tetrahydrofolypolyglutamate synthase domain, it was possible that SiFPGS2 could function in root development, we tested the root length of *SiFPGS2* over-expression lines. Firstly, *fpgs1* (SALK_032554c), *fpgs2* (SALK_008883c), *fpgs3* (SALK_038762c) T-DNA insertion mutant was ordered from Arashare corporation (http://arashare.cn), and the homozygous lines were tested by genomic PCR (Fig. S4). As in Fig. S5, after grown in white light chamber for 7 days, *fpgs2* mutant root length was shorter than Col-0, *fpgs3* show a little shorter than Col-0, while there was no significant difference between *fpgs1* and Col-0, so *fpgs2* mutant was chosen as control. The root length in *SiFPGS2* over-expressed lines reached 1.5 to 2 times compared to Col-0 (Fig. 5a, b), meanwhile the seedling weight in *SiFPGS2* over-expressed lines #3 reached 1.6 times compared to Col-0, while in #1 transgenic lines there were no significant difference, the result above suggested that *SiFPGS2* promote root development (Fig. 5c).

To further detect how *SiFPGS2* function in root development, propidium iodide (PI) staining was performed according that PI, a red-fluorescent nuclear stain, could not cross intact plasma membrane but could penetrate damaged or dead cells, so it could accumulate at the viabile cells membrane. The major root of Col-0 and *SiFPGS2* over-expressed lines grown in white light chamber for 4 days was cutted and stained with 180 μM PI, then the root architecture was detected by confocal, the root apical meristem zone length was measured and the division zone cell number was counted from the stem cell around the quiencent center to the cell that the cell length is the same as cell width in cortex (Fig. 6a), the result showed the root apical meristem zone length of Col-0, *fpgs2*, *35S::SiFPGS2*/Col-0 was 0.3, 0.22, 0.31 mm, respectively (Fig. 6b), and there were 42, 32, 44 cells of root apical meristem zone in wild type, *fpgs2* mutant and *SiFPGS2* over-express lines, respectively (Fig. 6c), which suggested that SiFPGS2 accelerated the root apical meristem zone cell division and promoted the root growth.

Discussion

Foxtail millet is rich in folates. Polyglutamylation of folates could enhance their compartmentalization, reducing their transport, increase their affinities with enzymes and increase the stability of the folate pool in *Arabidopsis*. The polyglutamylation reaction are catalyzed by FPGS. But FPGS function in foxtail millet is still elusive. In this study, we predicted that SiFPGS2 could catalyze the polyglutamylation of THF, and further verified its function in *35S::SiFPGS2*/Col-0 transgenic line, the results suggested that over-expression of SiFPGS2 in *Arabidopsis* leading to the increase of folates content and root length by promotion of root apical meristem zone cell division.

Prediction of SiFPGS2 gene function by bioinformation analysis

We collected three *SiFPGS* genes by blasted with AtFPGS1, AtFPGS2 and AtFPGS3 protein sequences, respectively. Interestingly, we got three same genes no matter which AtFPGS protein sequence was used for blast, which means that the three *SiFPGS* genes in foxtail millet were highly homologue to each other. The phylogenetic tree analysis suggested SiFPGS1, SiFPGS2 highly homologue to other FPGS in Gramineae species, and SiFPGS1, SiFPGS2 were near to each other than to other FPGS in dicots, such as AtFPGS, GmFPGS and SlFPGS; while SiFPGS3 belonged to DFA subfamily (Fig. 1). The protein function domain comparation showed that SiFPGS1, SiFPGS2 posessed the tetrahydrofolypolyglutamate synthase domain, SiFPGS3 possessed dihydrofolate synthase domain, this was in accordance with the result of phylogenetic tree analysis (Fig. S1). Docking analysis revealed that SiFPGS1, SiFPGS2 could bind THF as substrate, while SiFPGS3 could bind DHP, further supported the speculation that SiFPGS1, SiFPGS2 belong to the FPGS subfamily, and SiFPGS3 belong to DFA subfamily (Fig. 2, Fig. S2). Subcellular localization predicted that SiFPGS1, SiFPGS2 localized in the choloroplast (Table 1), this was in accordance with the result that AtFPGS3 localized in the chloroplast. It is predicted that SiFPGS3 localized extracellular (Table 1), Ravanel et al (2001) reported that AtDFA was localized in the mitochonidria, maybe there were different regulate mechanism among species and it will be verified in future. Cis-acting element prediction analysis showed that there were meristem expression motif and root specific motif in *SiFPGS2* promoter, which suggested that *SiFPGS*2 maybe take part in regulation of meristem formation and root development, this was in concert with the result that over-expressed *SiFPGS2* prolonged the root length by promoting root apical meristem zone cell division (Fig. 3, Table 2, Fig. 6). Taken together, the bioinformation assays indicated that SiFPGS2 was similar to SiFPGS1, belong to FPGS subfamily, catalyze the glutamylation of THF to produce polyglutamated THF, and SiFPGS3 belong to DFA subfamily, catalyze the first glutamate to DHP to produce DHF.

Over-expression of SiFPGS2 in Arabidopsis increasing folates content

For over-expression *SiFPGS2* gene in *Arabidopsis* increased folates content, we found that 5-CH_3-THF, 5-CHO-THF, 5,10-CH = THF and THF content were higher in the transgenic line, maybe over-expression of *SiFPGS2* in *Arabidopsis* kept more folates in the chloroplast, increased the stability of folates pool and enhanced the folates content (Fig. 4); meanwhile, we found that the content of DHF was decreassed in *SiFPGS2* over-expression line, this maybe owning to that in the reaction of SiFPGS2 catalyzing the production of polyglutamated THF, over-expressed *SiFPGS2* will consume more THF, then DHF as the

upstream subatrate of THF would be used more due to feedback, which would lead to the decrease the content of DHF (Fig. 4). From above results we deduced that over-expression of *SiFPGS2* in *Arabidopsis* kept more folates in the chloroplast, avoided folates from degradation and then increased the folates content.

Over-expression of SiFPGS2 in Arabidopsis increasing root length by promotion of root apical meristem cell division

For SiFPGS2 promoting major root elongation, we found that *SiFPGS2* over-expressed lines major root length was longer than Col-0, which suggested that *SiFPGS2* promoted root development (Fig. 5). In addition, we found there were no markable difference between *fpgs1* and Col-0 (Fig. S5), this was inaccordance with the result that *fpgs1*/ *atdfb* mutant root was obviously shorter than Col-0 (Srivastava et al. 2011a, Srivastava et al. 2011b), maybe *fpgs1* (SALK_032554c) mutant line, we ordered, was inserted in the last exon and might do not retain any FPGS1 activity; while *fpgs1*/ *atdfb* (SAIL_556_G08 and SALK_015472) mutants, they used in the papers, were inserted in the sixth intron and eighth exon, respectively, which might result in the generation of a truncated protein and attunation of FPGS1 activity. We found *fpgs2* mutant root length was shorter than Col-0 (Fig. S5), while Mehrshahi et al (2010) showed that their root length were the same as Col-0, maybe because that in their paper there were no sucrose in $^1/_2$ MS media, and in our experiment, the *Arabidopsis* seedlings were grown in $^1/_2$ MS media supplemented with 1% sucrose, which would supply more energy to promote the plant growth, consume more DNA and amino acids to accelarate cell division, in this case, there were no enough folates to synthesis DNA and amino acids in *fpgs2* mutant and showed short root.

For SiFPGS2 accelerating root apical meristem zone cell division, we found that *SiFPGS2* over-expressed lines with more root apical meristem zone cell number (Fig. 6), Srivastava et al (2011a) showed that the endogenous levels of adenine and guanosine were reduced in *atdfb*/ *fpgs1* mutant seedlings, maybe the increased folates content in *SiFPGS2* over-expressed lines accumulate more folates and then promote synthesis of adenine and guanosine, which supply more substrates for DNA replication and accelerate root apical meristem zone cell division, leading to the prolongation of root length.

Declarations

All the authors declared that they have no conflict of interest.

Author contribution statement

Yijuan Zhang and Siyu Hou designed the study and wrote the manuscript. Chongmei Zhang, Xiaxia Man, Lida Han and Xuemei Ren performed the experiments. Yihan Men, Xueyin Li and Yang Yang analyzed the data. Yuanhuai Han and Zhaoxia Sun supervised the research and modified the manuscript. All authors approved the final version of the manuscript.

Acknowledgments

We thank Lida Han in laboratory of Biotechnology Research Institute, Chinese Academy of Agricultural Sciences for measuring folate content. This work was supported by the National Natural Science Foundation of China (Grant number [32100316]); Joint Funds of the National Natural Science Foundation of China (Grant number [U21A20216]); Fundamental Research Program of Shanxi Province (Grant number [20210302123397]); National Key Research and Development Project (Grant number [2018YFD1000700/2018YFD1000706]); Youth Fund Project on Application of Basic Research Project of Shanxi Province (Grant number [201901D211363]).

References

1. Bennetzen JL, Schmutz J, Wang H, Percifield R, Hawkins J, Pontaroli AC, Estep M et al (2012) Reference genome sequence of the model plant *Setaria*. Nat Biotechnol 30(6):555–561. doi: https://doi.org/10.1038/nbt.2196
2. Besson V, Rebeille F, Neuburger M, Douce R, Cossins EA (1993) Effects of tetrahydrofolate polyglutamates on the kinetic parameters of serine hydroxymethyltransferase and glycine decarboxylase from pea leaf mitochondria. Biochem J 292(Pt 2):425–430. doi: https://doi.org/10.1042/bj2920425
3. Blancquaert D, Van Daele J, Strobbe S, Kiekens F, Storozhenko S, De Steur H, Gellynck X et al (2015) Improving folate (vitamin B9) stability in biofortified rice through metabolic engineering. Nat Biotechnol 33(10):1076–1078. doi: https://doi.org/10.1038/nbt.3358
4. De Lepeleire J, Strobbe S, Verstraete J, Blancquaert D, Ambach L, Visser RGF, Stove C et al (2018) Folate biofortification of potato by tuber-specific expression of four folate biosynthesis genes. Mol Plant 11(1):175–188. doi: https://doi.org/10.1016/j.molp.2017.12.008
5. Eckermann C, Eichel J, Schroder J (2000) Plant methionine synthase: new insights into properties and expression. Biol Chem 381(8):695–703. doi: https://doi.org/10.1515/BC.2000.090
6. Gorelova V, Ambach L, Rebeille F, Stove C, Van Der Straeten D (2017) Folates in plants: research advances and progress in crop biofortification. Front Chem 5:21. doi: https://doi.org/10.3389/fchem.2017.00021
7. Gregory JF, Quinlivan EP (2002) In vivo kinetics of folate metabolism. Annu Rev Nutr 22(22):199–200. doi: https://doi.org/10.1146/annurev.nutr.22.120701.083554
8. Hanson AD, Roje S (2001) One-carbon metabolism in higher plants.Annual Review of Plant Physiology and. Plant Mol Biol 52:119–137. doi: https://doi.org/10.1146/annurev.arplant.52.1.119
9. He L, Zhang B, Wang X, Li H, Han Y (2015) Foxtail millet: nutritional and eating quality, and prospects for genetic improvement. Frontiers of Agricultural Science and Engineering 2(2). 2015, 2(002):124–133
10. Hou S, Man X, Lian B, Ma G, Sun Z, Han L, Yan L et al (2022a) Folate metabolic profiling and expression of folate metabolism-related genes during panicle development in foxtail millet (*Setaria italica (L.) P. Beauv*). J Sci Food Agric 102(1):268–279. doi: https://doi.org/10.1002/jsfa.11355

11. Hou S, Zhang Y, Zhao B, Man X, Ma G, Men Y, Du W et al (2022b) Heterologous expression of SiFBP, a folate-binding protein from foxtail millet, confers increased folate content and altered amino acid profiles with nutritional potential to *Arabidopsis*. J Agric Food Chem 70(20):6272–6284. doi: https://doi.org/10.1021/acs.jafc.2c00357
12. Ishikawa T, Machida C, Yoshioka Y, Kitano H, Machida Y (2003) The *GLOBULAR ARREST1* gene, which is involved in the biosynthesis of folates, is essential for embryogenesis in *Arabidopsis thaliana*. Plant J 33(2):235–244. doi: https://doi.org/10.1046/j.1365-313x.2003.01621.x
13. Jagerstad M, Jastrebova J (2013) Occurrence, stability, and determination of formyl folates in foods. J Agric Food Chem 61(41):9758–9768. doi: https://doi.org/10.1021/jf4028427
14. Man X, Gao H, Yan L, Zhang Y, Sun Z, Han Y, Hou S (2020) Optimization of determination of folic acid in foxtail millet by HPLC. J China Agricultural Univ 1211. doi: https://doi.org/10.11841/j.issn.1007-4333.2020.12.12
15. Mcnulty H, Ward M, Hoey, Leane, Hughes CF, Pentieva K (2019) Addressing optimal folate and related B-vitamin status through the lifecycle: health impacts and challenges. Proceedings of The Nutrition Society 78(3): 1–14. doi:https://doi.org/10.1017/S0029665119000661
16. Mehrshahi P, Gonzalez-Jorge S, Akhtar TA, Ward JL, Santoyo-Castelazo A, Marcus SE, Lara-Nunez A et al (2010) Functional analysis of folate polyglutamylation and its essential role in plant metabolism and development. Plant J 64(2):267–279. doi: https://doi.org/10.1111/j.1365-313X.2010.04336.x
17. Orsomando G, De La Garza RD, Green BJ, Peng M, Rea PA, Ryan TJ, Gregory JF et al (2005) Plant gamma-glutamyl hydrolases and folate polyglutamates: characterization, compartmentation, and co-occurrence in vacuoles. J Biol Chem 280(32):28877–28884. doi: https://doi.org/10.1074/jbc.M504306200
18. Ravanel S, Cherest H, Jabrin S, Grunwald D, Surdin-Kerjan Y, Douce R, Rebeille F (2001) Tetrahydrofolate biosynthesis in plants: molecular and functional characterization of dihydrofolate synthetase and three isoforms of folylpolyglutamate synthetase in Arabidopsis thaliana. Proc Natl Acad Sci U S A 98(26):15360–15365. doi: https://doi.org/10.1073/pnas.261585098
19. Sachdev N, Goomer S, Singh LR (2021) Foxtail millet: a potential crop to meet future demand scenario for alternative sustainable protein. J Sci Food Agric 101(3):831–842. doi: https://doi.org/10.1002/jsfa.10716
20. Scott J, Rebeille F, Fletcher J (2000) Folic acid and folates: the feasibility for nutritional enhancement in plant foods. J Sci Food Agric 80(7):795–824
21. Shao L, Wang L (2014) Analysis of folic acid contents in main grain crops, fruits and vegetables. Food Sci 35(24):290–294. doi: https://doi.org/10.7506/spkx1002-6630-201424056
22. Shao L, Wang L, Bai W, Liu Y (2014) Evaluation and analysis of folic acid content in millet from different ecological regions in Shanxi Province. Scientia Agricultura Sinica 47(07):1265–1272
23. Srivastava AC, Ramos-Parra PA, Bedair M, Robledo-Hernandez AL, Tang Y, Sumner LW, De La Garza D et al (2011a) The folylpolyglutamate synthetase plastidial isoform is required for postembryonic root

development in *Arabidopsis*. Plant Physiol 155(3):1237–1251. doi: https://doi.org/10.1104/pp.110.168278

24. Srivastava AC, Tang Y, De La Garza RI, Blancaflor EB (2011b) The plastidial folylpolyglutamate synthetase and root apical meristem maintenance. Plant Signal Behav 6(5):751–754. doi: 10.4161/psp.6.5.15403
25. Strobbe S, Van Der Straeten D (2017) Folate biofortification in food crops. Curr Opin Biotechnol 44:202–211. doi: https://doi.org/10.1016/j.copbio.2016.12.003
26. Wan X, Han LD, Yang M, Zhang HY, Zhang CY, Hu P (2019) Simultaneous extraction and determination of mono-/polyglutamyl folates using high-performance liquid chromatography-tandem mass spectrometry and its applications in starchy crops. Anal Bioanal Chem 411(13):2891–2904. doi: https://doi.org/10.1007/s00216-019-01742-0
27. Wang L, Kong D, Lv Q, Niu G, Han T, Zhao X, Meng S et al (2017) Tetrahydrofolate Modulates floral transition through epigenetic silencing. Plant Physiol 174(2):1274–1284. doi: https://doi.org/10.1104/pp.16.01750
28. Yang Z, Zhang H, Li X, Shen H, Gao J, Hou S, Zhang B et al (2020) A mini foxtail millet with an *Arabidopsis*-like life cycle as a C4 model system. Nat Plants 6(9):1167–1178. doi: https://doi.org/10.1038/s41477-020-0747-7
29. Yu J, Qiu H, Liu X, Wang M, Gao Y, Chory J, Tao Y (2015) Characterization of tub4(P287L), a beta-tubulin mutant, revealed new aspects of microtubule regulation in shade. J Integr Plant Biol 57(9):757–769. doi: https://doi.org/10.1111/jipb.12363
30. Zhang G, Liu X, Quan Z, Cheng S, Xu X, Pan S, Xie M et al (2012) Genome sequence of foxtail millet (*Setaria italica*) provides insights into grass evolution and biofuel potential. Nat Biotechnol 30(6):549–554. doi: https://doi.org/10.1038/nbt.2195
31. Zhang Y, Wen C, Liu S, Zheng L, Shen B, Tao Y (2016) Shade avoidance 6 encodes an *Arabidopsis* flap endonuclease required for maintenance of genome integrity and development. Nucleic Acids Res 44(3):1271–1284. doi: https://doi.org/10.1093/nar/gkv1474

Figures

Figure 1

Phylogenetic analysis, conserved domains and gene structure of *FPGS* genes from different species. The genes are as follows: SiFPGS1 (*Setaria italica,* Seita.9G200900), SvFPGS1 (*Setaria viridis,* Sevir.9G200100), SbFPGS1 (*Sorghum bicolor,* Sobic.001G201900), ZmFPGS1 (*Zea mays,* ZmB84.K044900), OsFPGS1 (*Oryza sativa,* Os10g35940), OsFPGS2 (*Oryza sativa,* Os03g02030), SiFPGS2 (*Setaria italica,* Seita.9G571100), SvFPGS2 (*Setaria viridis,* Sevir.9G574400), SbFPGS2 (*Sorghum bicolor,* Sobic.001G535500), ZmFPGS2 (*Zea mays,* ZmB84.09G254000), AtFPGS3 (*Arabidopsis thaliana*, AT3G55630), GmFPGS1 (*Glycine max*, Glyma.02G251400), GmFPGS2 (*Glycine max*, Glyma.14G065400), SlFPGS1 (*Solanum lycopersicum* L., Lm.05g052920), AtFPGS1 (*Arabidopsis thaliana*, AT5G05980), AtFPGS2 (*Arabidopsis thaliana*, AT3G10160), GmDFA (*Glycine max*, Glyma.10G065800), SlDFA (*Solanum lycopersicum* L., Lm.06g051900), AtDFA (*Arabidopsis thaliana*, AT5G41480), OsFPGS3 (*Oryza sativa,* Os12g42870), SiFPGS3 (*Setaria italica,* Seita.2G382200), SvFPGS3 (*Setaria viridis,* Sevir.2G392500), SbFPGS3 (*Sorghum bicolor,* Sobic.008G125100), ZmFPGS3 (*Zea mays,* ZmB84.10G043600)

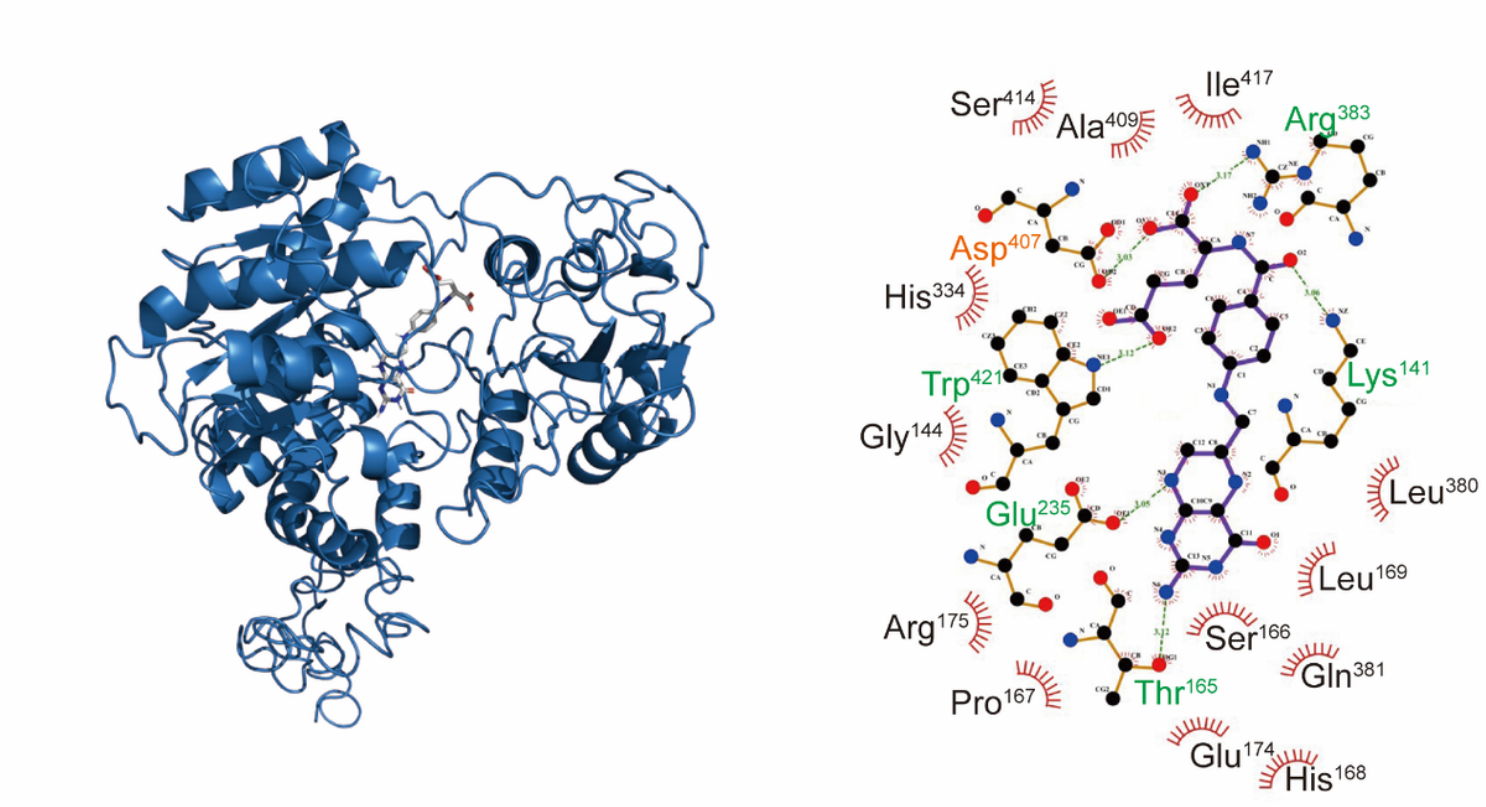

Figure 2

Molecular docking analysis of SiFPGS2 and THF. Amino acid in black indicated hydrophobic interaction between SiFPGS2 and THF, amino acid in green indicated hydrogen bonds, and amino acid in orange indicated electrostatic interaction.

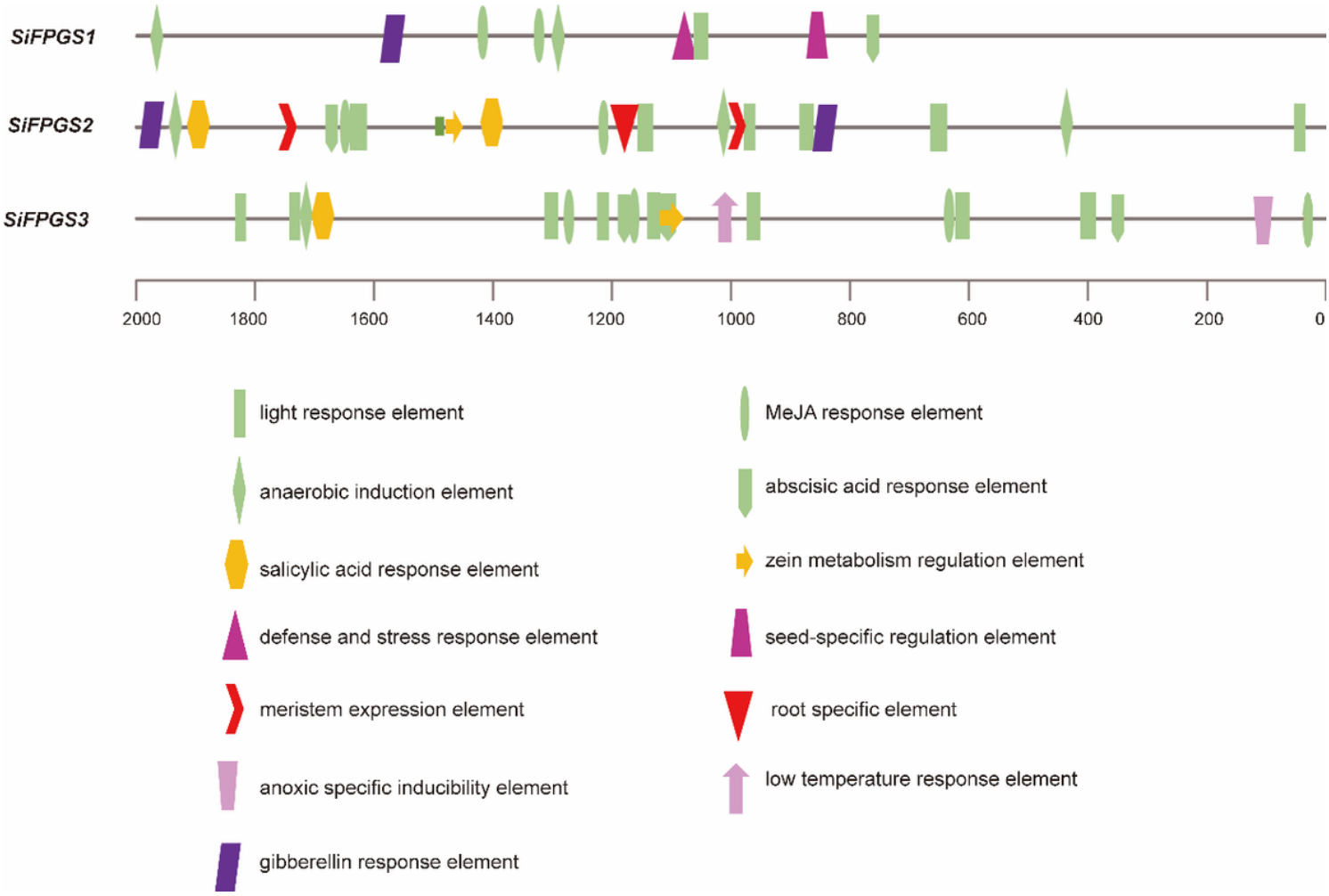

Figure 3

Cis-acting elements analysis of *SiFPGS* genes family of foxtail millet.

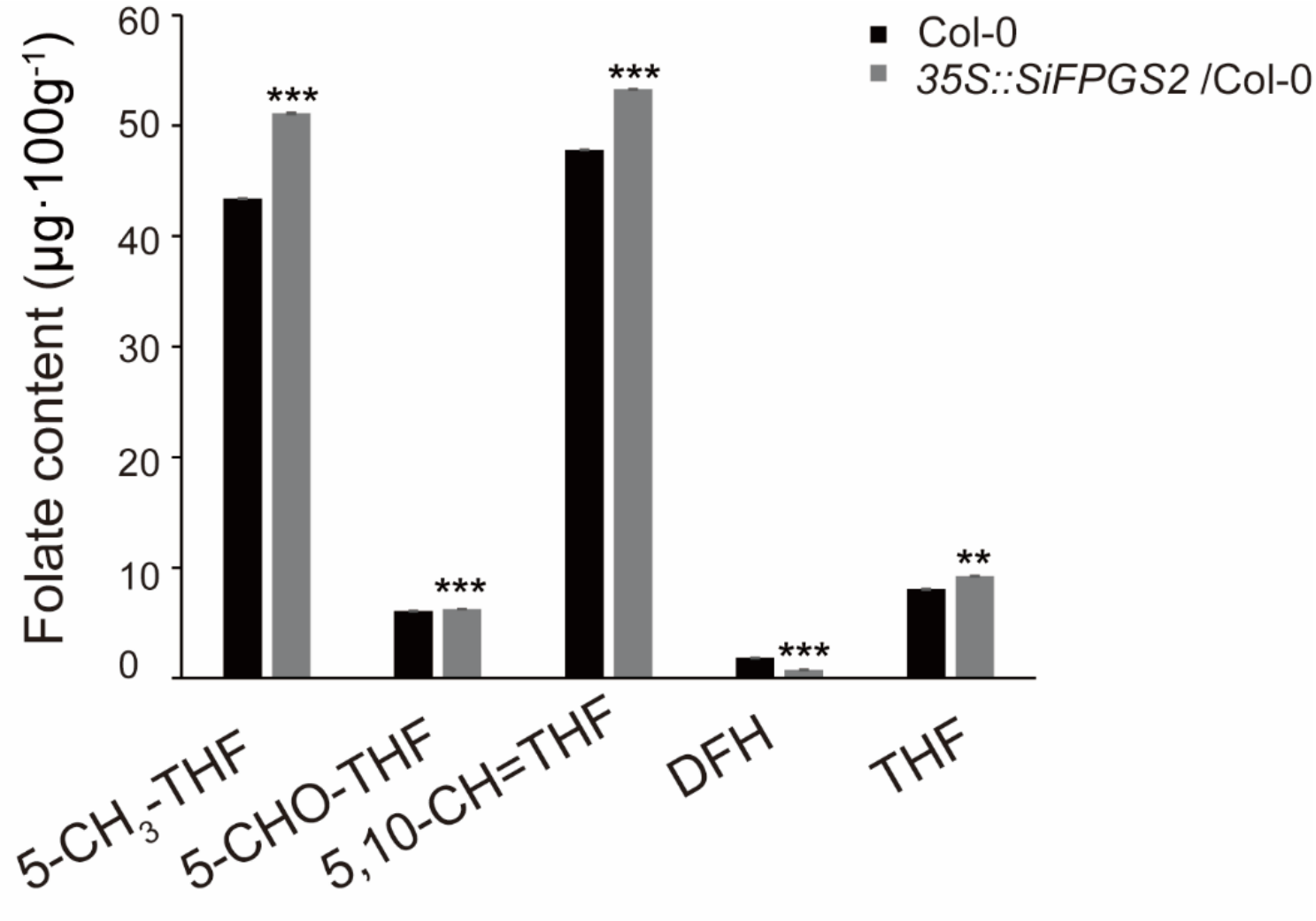

Figure 4

Folates content analysis in wild type *Arabidopsis* and *SiFPGS2* over-expression line. The 5th-7th rosette leaves one month old of wild type and over-expression lines were harvested and the folates content were measured, respectively. 5-CH_3-THF, 5-methylene-tetrahydrofolate; 5-CHO-THF, 5-formyl-tetrahydrofolate; 5,10-CH=THF, 5,10-methylene-tetrahydrofolate; DHF, dihydrofolate; THF, tetrahydrofolate. Note: the error bars indicate standard error. "**" means significant difference at 0.001<P<0.01， "***" means significant difference at P<0.001.

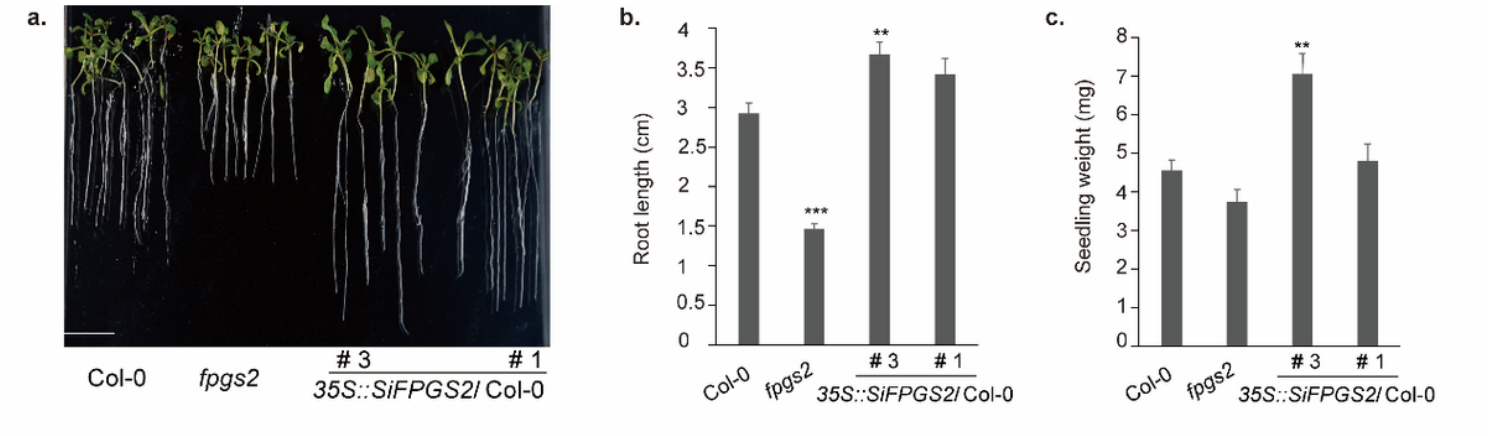

Figure 5

Phenotype of *SiFPGS2* over-expressed lines in *Arabidopsis*. a. Phenotype comparation of Col-0, *fpgs2*, *35S::SiFPGS2*/Col-0 grown in erected $^{1}/_{2}$ MS for 7 days. The bar represents 1cm. **b.** The root length comparation of Col-0, *fpgs2*, *35S::SiFPGS2*/Col-0. **c.** The seedling weight comparation of Col-0, *fpgs2*, *35S::SiFPGS2*/Col-0. Note: the error bars indicate standard error. "**" means significant difference at 0.001<P<0.01.

Figure 6

Over-expressed *SiFPGS2* in *Arabidopsis* promote root apical meristem length and cell division. a. Root apical meristem zone construction comparation among Col-0, *fpgs2* and *35S::SiFPGS2*/Col-0. The white line indicated the division zone in the root. The bar represents 0.5μm. **b.** Root apical meristem zone length comparation among Col-0, *fpgs2* and *35S::SiFPGS2*/Col-0. the length was measured according the white line in figure A. **c.** Root apical meristem zone cell number comparation among Col-0, *fpgs2* and *35S::SiFPGS2*/Col-0. Note: the error bars indicate standard error. "***" means significant difference at *P*<0.001.

Supplementary Files

This is a list of supplementary files associated with this preprint. Click to download.

- phylogenetictreedata.doc
- supplementarymaterial.docx